Ceramics International 46 (2020) 29120–29129

Contents lists available at ScienceDirect

Ceramics International

journal homepage: www.elsevier.com/locate/ceramint

A study on optimum surfactant to multiwalled carbon nanotube ratio in alcoholic stable suspensions via UV–Vis absorption spectroscopy and zeta potential analysis

Ali Can Zaman[a,*], Figen Kaya[b], Cengiz Kaya[c,d]

[a] Yıldız Technical University, Science and Technology Application and Research Center, 34200, Istanbul, Turkey
[b] Yıldız Technical University, Faculty of Chemistry and Metallurgy, Department of Metallurgical and Materials Engineering, Istanbul, 34200, Turkey
[c] Sabancı University, Faculty of Engineering and Natural Sciences, Materials Science and Nano Engineering, 34956, Istanbul, Turkey
[d] Sabancı University, Nanotechnology Research and Application Centre (SUNUM), 34956, Istanbul, Turkey

ARTICLE INFO

Keywords:
UV–Vis absorption spectroscopy
Dispersion
Carbon nanotube
Colloid
Quantitative
Surfactant

ABSTRACT

Common ultrasonication and centrifugation techniques could be utilized for dispersion of carbon nanotubes in solvents. However, there are few studies investigating the effect of concentration of species on stability of surfactant modified suspensions focusing on specific dispersants. Therefore, in this study, UV–Vis absorption spectroscopy, sedimentations tests, zeta (ζ) potential and dynamic light scattering analyses (DLS) were used as tools to estimate the optimal surfactant to multi walled carbon nanotubes (MWCNTs) weight ratio in stable centrifuged suspensions. MWCNTs colloids were prepared via addition of sodium dodecylbenzene sulfonate (SDBS) with ultrasonication and centrifugation in isopropyl alcohol (IPA). Coupling information gathered from overlapped absorption spectra and weighed dried sediments enabled estimation of MWCNTs concentrations in centrifuged suspensions (supernatant). By utilizing sediments weight and zeta potential observations, optimum SDBS/MWCNTs weight ratios were calculated. The results have shown that the SDBS/MWCNTs ratio should be 9 or higher in supernatants in order to obtain stable suspensions. It was also observed that increasing SDBS/MWCNTs concentrations over 9 in supernatants gradually decreased the zeta potentials of studied suspensions. Higher SDBS/MWCNTs ratios, also decreased settling velocities that were attributed to increased viscosity of supernatants. In addition to overlapping spectra technique, which relies on utilization of spectra related to centrifuged and uncentrifuged suspensions only for quantitative analysis, differential UV–Vis spectra were also utilized for the assessment of SDBS/MWCNTs ratios in supernatants. Presence of SDBS in supernatants (prepared by removing contribution of MWCNTs by using COOH modified MWCNTs' UV–Vis absorption spectrum) exhibited an unexpected hyperchromic shift in maximum wavelength in spectra leading to misleading estimations of surfactant concentrations.

1. Introduction

Carbon nanotubes (CNTs) are outstanding materials and suitable to be used as a conductive filler or reinforcement material in composites [1–3]. The rapid progress in carbon nanotube research particularly in the last three decades raised the need for ease of manipulation of these novel materials. For example, carbon nanotube reinforced composite production requires a mixing step mostly in liquid environments. However, obtaining stable liquid suspensions in which CNTs present as individual entities is not straightforward. Particularly in polar solvents, preventing entanglement/agglomeration of CNTs is difficult because of Wan der Waals inter-tube binding that could reach up to 500 eV per micrometer [4].

Various approaches could be employed in the processes of liquid phase dispersion of CNTs. The most straightforward approach is achieving stability by using an appropriate solvent. In this respect, spectrum of solvents is limited, such as use of CHP (cyclohexyl-pyrrolidone) and dimethylformamide (DMF) that are successful for single walled SWCNTs [5]. These solvents are generally known to be toxic and require special care during usage and disposal. There can be additional drawbacks, for example, DMF was found to damage the structure of SWCNTs [6]. In another perspective, surface properties of carbon nanotubes changes with their diameter. The interaction between carbon nanotubes' surface and dispersants/solvents is dependent on curvature

* Corresponding author.
E-mail address: aczaman@yildiz.edu.tr (A.C. Zaman).

https://doi.org/10.1016/j.ceramint.2020.08.085
Received 29 May 2020; Received in revised form 10 August 2020; Accepted 11 August 2020
Available online 16 August 2020
0272-8842/ © 2020 Elsevier Ltd and Techna Group S.r.l. All rights reserved.

of the graphene sheets. Thus, it should be noted that solvents working properly with SWCNTs may not function well with MWCNTs [7]. Second approach for rendering nanotubes to be dispersible is covalently attaching functional groups by post treatments [8]. Although this approach works well, it causes severe drawbacks on properties of nanotubes [9]. Non-covalent functionalization is the third method which is based on adsorption of molecules on the CNT surface. Therefore, for this purpose surfactants [10,11], polymers [12], biomacromolecules (saccharides, polysaccharides, proteins, enzymes, DNA) and aromatic molecules [13] are used. Unwanted materials in suspensions are drawbacks in composite structures notwithstanding, with the aid of dispersants; non-toxic and cheap solvents could be used, such as water or IPA (isopropyl alcohol). SDBS is a well-known surfactant widely used in dispersion studies of carbon nanotubes in the literature. The benzene ring in its structure provides π-π stacking interaction with carbon nanotube surface, hence it may provide electrostatic stability in aqueous suspensions [14]. Utsumi et al. found that there is a strong interaction between SDBS and CNTs [15]. It is also concluded that dispersion concentration of up to 20 mg mL^{-1} for CNTs could be achieved in aqueous CNTs solutions with use of SDBS [16]. Furthermore, depending on the application, selection of appropriate solvent is also crucial. For instance, conducting electrophoretic deposition (EPD) under relatively high voltages ($\geq$4V) with direct current dictates use of non-aqueous solvents, and surfactants that could work effectively in organic solvents for achieving non-covalent functionalization. Therefore, it is also possible to prepare surfactant stabilized CNT suspensions in organic solvents.

As well as selection of surfactant type, surfactant concentration is also a critical factor in obtaining stable suspensions. Excess amount of surfactant may severely affect final structure of composite after consolidation at high temperatures. Because during consolidation processes, such as spark plasma or vacuum sintering, surfactant molecules may cause formation of pores/bubbles leading to localized stress concertation sites in the final composite structure.

Once the stable suspension is obtained with an appropriate method, a second problem arises which is dependent on the dispersion steps used. If dispersion after ultrasonication is followed by centrifugation, henceforth, information about carbon nanotube and dispersant concentration is lost in supernatant. This data is important for one to comprehensively understand the effect of materials quantity over composite properties. In this context, UV–Vis absorption spectroscopy could be used to determine material concentration in suspensions. UV–Vis absorption spectroscopy has long been utilized on carbon nanotubes by researchers to determine dispersion efficiency [17,18], to evaluate interaction behavior between carbon nanotubes and dispersants [19,20], impurity analysis [21] and concentration determination [22,23]. This method is notable because it enables characterization in liquid state [17]. Some important publications on the subject are as follows: Jeong et al. determined concentration of SWCNTs in aqueous suspensions by measuring absorbance once the extinction coefficient was determined in advance [24]. Bahr et al. used a calibration curve for SWCNTs by weighing ultrasonicated SWCNTs sediments and combined these data with UV–Vis information [25]. There are some attempts in the literature to find optimum concentration of carbon nanotubes in supernatants using UV–Vis spectroscopy [18]. But the actual surfactant and SWCNTs concentrations in the supernatant are not taken in to account as the centrifugation step is omitted. Attal et al. [22] successfully introduced UV–Vis spectroscopy to determine material concentration in centrifuged samples using subtracted spectra or overlapped spectra of multicomponent system of SDBS/SWCNTs. Fernandes et al. [26] combined TGA and UV–Vis spectroscopy in an attempt to quantitatively analyze surfactant concentration in stabilized carbon nanotube dispersions. In our previous article we also utilized overlapping spectra of CNTs and differentiated spectra of PVP in IPA as to determine polymer and MWCNTs concentrations in centrifuged suspensions [27]. Suspensions prepared by keeping concentration value of one component constant while the other is being altered may yield information about dispersion power of the surfactant and optimum CNT to surfactant ratio by utilization of UV–Vis spectra [11]. But if one wants to gather the information to understand the concentration of solid content in centrifuged suspensions, different approaches should be implemented.

Another aspect needs to be understood is dispersion efficiency. Dispersion efficiency could be evaluated by using various techniques. For example, zeta (ζ) potential analysis [26,28,29], UV–Vis spectroscopy [30–33], optical microscopy [34], optical analyzers [28] and AFM [10] as well as SEM and TEM [15] could be used for this purpose. Zeta potential is a convenient tool and gives valuable information about the charges (magnitude of electrical double layer) around particles which are accounting for repulsion between similarly charged particles and hence indicates degree of dispersion efficiency. Combining zeta potential measurements with UV–Vis spectroscopic results could yield valuable information in finding optimized dispersant to CNTs ratio.

Based on given information, the need of a comprehensive approach for characterization of MWCNT containing colloids by combining various techniques is still valid. Accordingly, the aim of this paper is to analyze MWCNTs suspensions for understanding fundamental factors on stability of suspension. UV–Vis spectroscopy, sedimentation tests, zeta potential measurements and dynamic light scattering analysis are employed on MWCNTs suspensions dispersed with the aid of a well-known surfactant to comprehensively reveal the factors related to concentration of components affecting suspension stability.

2. Experimental methods

2.1. Preparation of MWCNTs suspensions

Sodium dodecyl benzene sulfonate (SDBS) was supplied from Sigma Aldrich (289957). MWCNTs were purchased from Thomas Swan Co. Ltd. with the average diameter and length of 30 nm and 30 μm, respectively. IPA was supplied from Merck (1.09634.2500). Pristine MWCNTs were mixed with SDBS in IPA. In the first series of experiments, SDBS concentrations were kept constant at 2 g L^{-1}. MWCNTs concentrations were varied between 0.1 g L^{-1} to 0.5 g L^{-1}. Hence, SDBS/MWCNTs weight concentration ratios were 20, 10, 6.6, 5 and 4 prior to mixing. In other two suspensions MWCNTs concentrations were kept at 0.4 g L^{-1} and 0.5 g L^{-1}. In these suspensions SDBS/MWCNTs weight concentration ratio was 7. Ultrasonication was implemented using Bandelin Sonorex HD 3100 with a KE76 tip (20% amplitude) for 1 h. Glass bottles containing 60 ml of suspensions were immersed in an ice bath. Therefore, the temperature of the suspensions was kept at 0 °C. There are two reasons behind keeping the samples cool during ultrasonication; firstly solvent removal by the heat is prevented and secondly dispersion state of carbon nanotubes can be enhanced at relatively low temperatures [18]. Subsequent to ultrasonication, centrifugation was implemented at 12000 relative centrifugal force (RCF) for 30 min at 20 °C for each suspension. Immediately after centrifugation, supernatants were decanted (10 mL was withdrawn from each centrifuge tube having 30 mL liquid). Precipitates were weighed and recorded after drying in an oven (700 mBar, 70 °C). 5 mL of each suspension was taken and used in sedimentations tests by keeping them in rest. Labeling of suspensions were done using initial concentration values and names of materials in suspensions. Namely, initially 0.1 g L^{-1} MWCNTs and 2 g L^{-1} SDBS containing suspension was designated as 0.1MWCNTs2SDBS. Uncentrifuged suspensions were labeled with “CF” letters.

2.2. SEM analysis

After implementation of ultrasonication, centrifugation and decantation, a representative sample was analyzed by scanning electron microscopy (SEM). High magnification SEM images were obtained with

JEOL 7000F field emission electron microscope (FE-SEM) to show diameter distribution of MWCNTs. Diluted centrifuged/decanted suspension was prepared and dried on silicon wafer, which was imaged with Zeiss EVO LS 10 to show the length distribution of fragmented MWCNTs.

2.3. UV–vis spectroscopy of MWCNTs suspensions

PGeneral T80+ UV–Vis spectrophotometer was utilized to obtain absorption spectra of suspensions. Resolution was kept at 1 nm. A single quartz cuvette having a 3500 μL chamber volume (Hellma Analytics) was used. Prior to each experiment background subtraction was carried out by using pure IPA. All suspensions were diluted with pure IPA before measurements. Scaling spectra of different suspensions at the same absorbance height at appropriate wavelengths were conducted to determine MWCNTs concentrations in suspensions. Namely, spectra of centrifuged suspensions were overlapped with those of uncentrifuged ones in the visible and infrared region where only carbon nanotubes are contributing to absorption. Two types of SDBS concentration calculation techniques are employed. In the first attempt, SBDS concentration calculation was carried out by using dried sediment weights (i) and concentration values of MWCNTs in centrifuged suspensions (ii) (obtained by utilizing overlapping spectra of centrifuged and uncentrifuged suspensions as aforementioned). After decantation of supernatants, centrifuge tubes were kept upside down and placed in an oven (70 °C), sediments were weighed subsequent to total drying. Second technique to calculate SDBS concentration required a different set up. Carboxyl group modified carbon nanotubes (COOH/MWCNTs) were obtained by treatment of 0.1 g L^{-1} MWCNTs in strong acid solution (3/1 Vol% H_2SO_4 and HNO_3) in an ultrasonic bath for 3h at 45°C. COOH/MWCNTs were obtained after filtration and drying steps. COOH-MWCNTs suspensions were prepared by ultrasonication and centrifugation in IPA. And 1 g L^{-1} SDBS containing suspensions in IPA was prepared for the purpose of plotting calibration curve of SDBS in IPA. SDBS suspension was properly diluted with pure IPA and absorption spectra were recorded between 0.005 g L^{-1} and 0.04 g L^{-1}. Finally, overlapped spectrum of COOH/MWCNTs was subtracted from those of SDBS/MWCNTs. After subtraction of contribution of MWCNTs from SDBS/MWCNTs spectra, “bound spectra” of SDBS in MWCNTs environment were obtained for each suspension/supernatant. A calibration curve and bound spectra of SDBS were utilized to determine SDBS concentrations.

2.4. ζ Potential and particle size measurements

A zeta potential and particle size analyzer (Malvern Zetasizer Nano ZS) was employed to quantitatively determine stabilities of suspensions. DTS 1070 sample cuvettes were used for both zeta potential and particle size analysis. Zetasizer measures velocity of the particles in the suspension through electrophoretic light scattering (ELS) principle. Then electrophoretic mobility (μ) is calculated by considering electric field strength, and the measured electrophoretic mobility data converted into zeta potential through Henry equation below (1):

$$\mu = \frac{2\varepsilon\zeta f(\kappa\alpha)}{3\pi\eta} \quad (1)$$

ε = is dielectric constant of the solvent, ζ is zeta potential, η is viscosity and f (κα) is Henry function. α is particle diameter and κ is refered to as the Debye parameter and it can be calculated from the electronic charge, Boltzmann's and Avagadro's constants, the absolute temperature and the ionic strength [35]. Ionic strength can be calculated from the pH of the suspension. 1/κ is acknowledged as “thickness” of the electrical double layer (the Debye length) and thus the units of κ are reciprocal length. Therefore f (κα) is dimensionless and usually assigned to the value of 1.00 or 1.50 [35]. Double layer thickness or Debye length is inversely proportional to the square root of ionic strength. Presence of ions suppresses the thickness of the double layer. In polar media such as in aqueous environments double layer thickness is very thin compared to particle diameter and f (κα) is taken 1.5, which is Smoluchowski's approximation. In contrast, in non-polar media Huckel's approximation is used where f (κα) is taken 1. Generally solvents having dielectric constants lower than 20 are considered non-polar, hence Huckel's approximation was chosen in calculation processes of zeta potentials in this study since IPA can be considered a non-polar solvent. Dielectric constant, refractive index and viscosity of IPA was taken as 19.3, 1.378 and 2.016 cP, respectively. All measurements were carried out under 150 V potential difference and at 25 °C. For concentrated samples, zeta runs for each measurement was set equal or more than 100 to increase the reproducibility, whereas zeta-run for dilute samples was kept as 50. Measurement position was 2 mm for all measurements. An automatic attenuator selection was employed.

Dynamic light scattering measurements were conducted in order to determine particle size distribution of MWCNTs and SDBS suspensions. Since MWCNTs suspensions are very opaque, suspensions were diluted before each measurement. Dilution was conducted by using pure IPA. Refractive index of MWCNTs was taken as 2.42 and absorbance was set to 1. Duration for each measurement was 100 s.

3. Results and discussion

3.1. Structural analysis and sedimentation tests

FE-SEM images of MWCNTs confirms that diameter of MWCNTs is about 30 nm (Fig. 1a and inset). After relatively long tip sonication, it seems that MWCNTs become fragmented and bundled (Fig. 1b). The length distribution of fragmented MWCNTs is broad ranging from tens of nanometers to several micrometers. This result will be corroborated with DLS analysis in the following sections. In pristine form MWCNTs aggregate in IPA. SDBS modified MWCNTs in IPA could exhibit high stability depending on SDBS/MWCNTs mass ratio. At a fixed initial SDBS concentration (before centrifugation), increasing MWCNTs concentration up to 0.3 g L^{-1} may allow retaining long term stability as shown in Fig. 1c. 0.1MWCNTs2SDBS, 0.2MWCNTs2SDBS and 0.3MWCNTs2SDBS supernatants are stable for months after ultrasonication and centrifugation. 0.3MWCNTs2SDBS is stable slightly more than 3 months. For concentration values between 0.3 and 0.5 g L^{-1}, increasing the amount of MWCNTs in suspensions increased sedimentation rates as a result these supernatant suspensions precipitated within 2 weeks.

It was assumed that initial SDBS or MWCNTs weights could be associated with concentration of components remaining in the solution after centrifugation. Thereby two requirements were acknowledged as satisfied with 0.3MWCNTs2SDBS by considering sedimentation tests and initial masses of MWCNTs: retaining relatively high MWCNTs concentration in supernatant and possession of low sedimentation rate/stability. By acting upon this assumption, 0.4MWCNTs2.8SDBBS and 0.5MWCNTs3.5SDBS were prepared. Interestingly, these suspensions turned out to be even more stable than 0.3MWCNTs2SDBS according to sedimentation tests. They remain stable for more than 6 months. If solid content concentration is increasing in the suspension, this obviously leads to a higher probability of particle collisions and agglomeration due to confined places in liquid. However, it is also possible that viscosity may take over the sedimentation behavior. After about a year, all suspensions have precipitated by having a transparent region at the top and black slurries at the bottom. Additionally, some of the suspensions have shown a yellowish hue at the top regions. It may be the result of severe sonication generated radicals that caused polymerization of SDBS molecules [36].

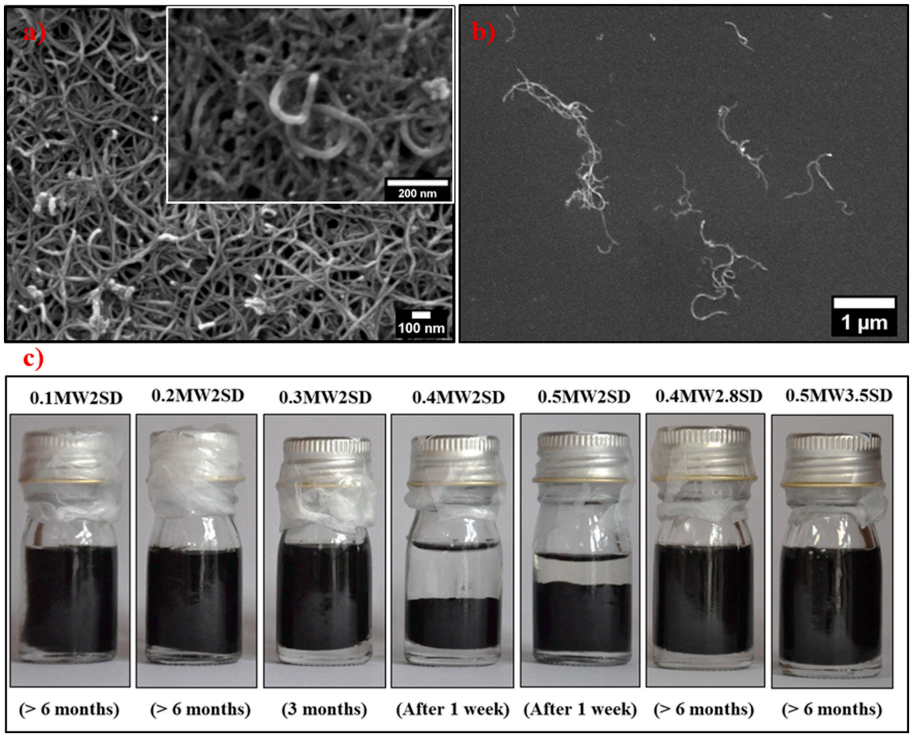


Fig. 1. a) FE-SEM image of MWCNTs (inset is high magnification micrograph), b) SEM image of MWCNTs subjected to probe sonication, which led to fragmentation, c) sedimentation test results of dispersions of MWCNTs with the aid of SDBS in IPA after ultrasonication and centrifugation. Time data below the images show the duration of sedimentation test for respective suspension.

3.2. Determination of SDBS and MWCNTs concentration by overlapping UV–Vis spectra

Schematic of sequence of events related to determination of surfactant and CNT concentration in centrifuged suspensions is shown in Fig. 2.

Remaining nanotubes in supernatants could be easily determined by using absorption spectroscopy as studied in literature by several authors [27,37,38]. But some aspects should be clarified in order to determine the reliability of use of UV–Vis spectroscopy. It is needed to be understood that whether light absorption of MWCNTs is affected by the presence of dispersants. Surfactants or polymers having aromatic rings in their structure interacts with nanotubes via π-π stacking interactions which is beneficial for stabilization. However, this interaction can perturb CNT electronic states, therefore UV–Vis absorption behavior may be influenced [20]. For example, Karachevtsev et al. stated that hypochromic shift is observed in the 300–400 nm spectral region of the absorbance spectrum of single walled carbon nanotubes (SWCNTs) which is the result of π-π stacking interaction of dispersant with nanotube surface [19]. To this end, if two suspensions were to be compared and if MWCNTs in these suspensions were influenced differently from π-π stacking interactions due to the difference in concentrations of interacting SDBS molecules, quantitative information may not be gathered. Namely, adsorption of surfactants may follow four stage adsorption model: (i) adsorption of isolated surfactants at low concentrations, (ii) formation of surfactant monolayer, (iii) formation of micelles on the surface, (iv) formation of micelles in the bulk [34]. In different stages, SDBS concentration may give different shifts in MWCNTs spectra. Therefore, the effect of difference in surfactant to MWCNTs mass concentrations on electronic properties should be evaluated. CNTs exhibit broad absorptions at the UV region due to Plasmon resonances in the free electron cloud of π electrons [39] and this adsorption has a long tail extending beyond near infrared region of the spectrum (indicated by dashed region in spectra in Fig. 3a). It is known that this absorption tail in UV–vis–NIR is solely due to MWCNTs. By utilizing this information, UV–Vis absorption spectra of suspensions: 0.1MWCTNs2SDBS CF, 0.3MWCTNs2SDBS CF and 0.5MWCTNs2SDBS CF are scaled to same level as shown in Fig. 2a. These suspensions were selected because spectrum of SDBS/MWCNTs mass ratios range from relatively low (SDBS/MWCNTs: 4) to high (SDBS/MWCNTs: 20). It is understood that at least by keeping SDBS/MWCNTs mass ratio between 20 and 4, may give convenient results if one wants to determine MWCNTs concentrations by using overlapping spectra or by using a calibration curve. Fig. 3b shows spectra of centrifuged SDBS/MWCNTs suspensions and an uncentrifuged suspension: 0.1MWCNTs2SDBS CF. MWCNTs concentrations in supernatants were calculated from these overlapped spectra.

In Table 1, concentration of MWCNTs, measured weight of materials precipitated after centrifugation and calculated SDBS concentrations are tabulated. Derived values of SDBS/MWCNTs mass concentration ratios are presented along with initial concentration ratios in Table 1 as well. With the help of information of dry sediment weights, simple arithmetic $((\text{SDBS} + \text{MWCNTs})_{\text{uncentrifuged suspension}} = (\text{SDBS} + \text{MWCNTs})_{\text{supernatant}} + (\text{SBDS} + \text{MWCNTs})_{\text{sediment}})$ were utilized to obtain SDBS concentration in supernatants. Concentration assessment can also be done by drawing a calibration curve, but process becomes easier, especially if double slit spectrometer is used and when serially diluted suspension are being evaluated.

Results indicate that the ratio between initial and final MWCNTs concentrations after ultrasonication vary from 1.7 to 2.12 (It could be calculated by using data in Table 1). Results also revealed that as MWCNTs concentration increases, SDBS concentration tends to decrease in supernatants, and it also reaches a plateau value (around 1.4 g L^{-1}). Because SDBS concentrations of 0.4MWCNTs2SDBS (1.37 g L^{-1}) and 0.5MWCNTs2SDBS (1.37 g L^{-1}) are marginally different. Another thing to consider is encountered during sediment weight evolution processes. Precipitate hardness and stickiness can be an indication of the suspensions stability.

Final weight concentration ratios of 0.3MWCNTs2SDBS, 0.4MWCNTs2.8SDBS and 0.5MWCNTs3.5SDBS are quite similar. It is known through sedimentation tests that these suspensions can be considered stable. Thus, it can be put forward that particularly under this preparation conditions for suspensions of MWCNTs having 30 nm of diameters in isopropyl alcohol, stability in supernatants could be

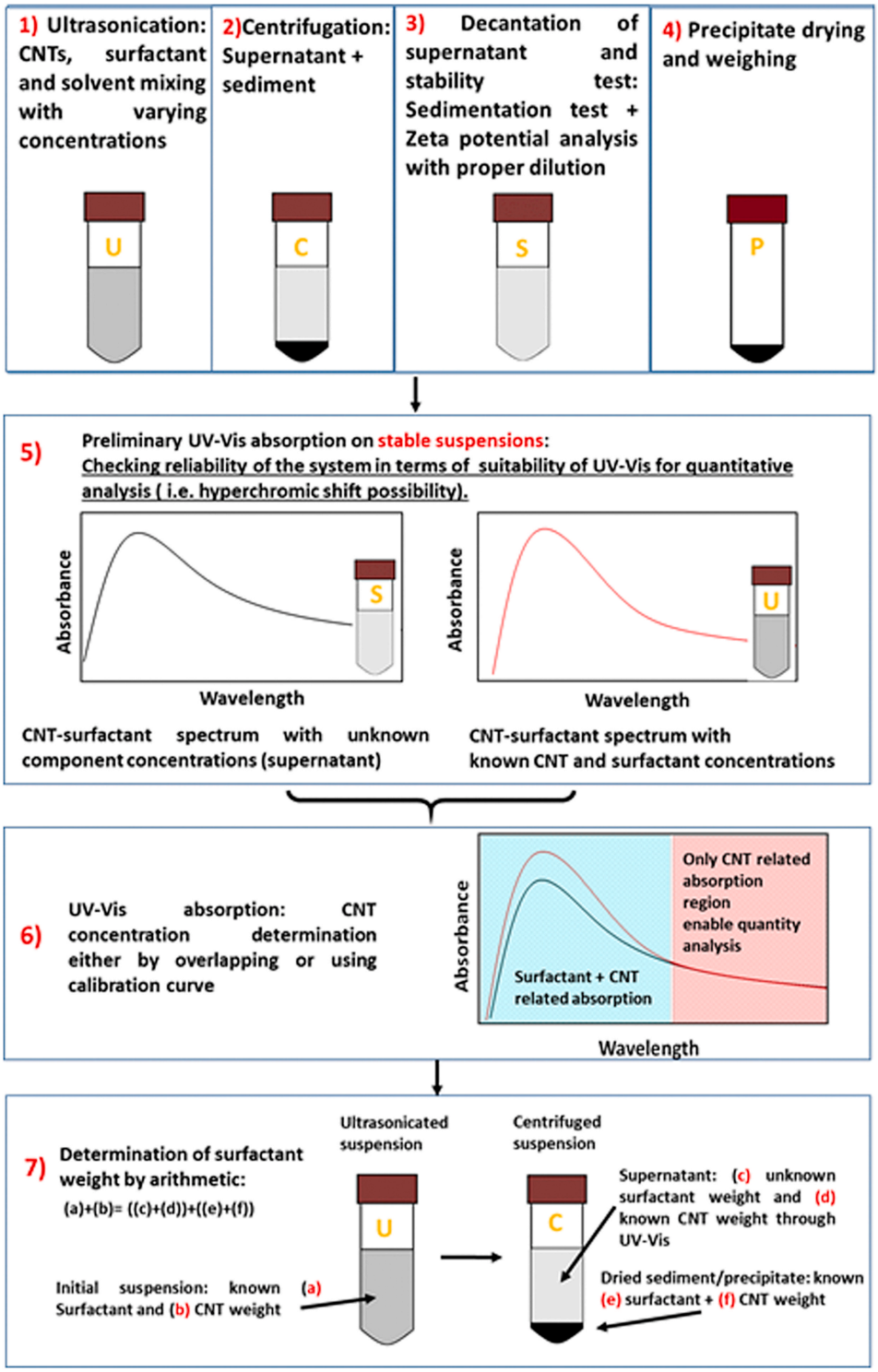


Fig. 2. Schematic showing the sequence of events implemented to determine the MWCNTs and surfactant concentration in supernatants.

maintained by keeping SDBS/MWCNTs weight concentration ratio around 7 before centrifugation, which yields a weight concentration ratio of 10 in supernatants. This finding may not be restricted, but certain if MWCNTs concentration in uncentrifuged suspension is below or equal to 0.5 g L^{-1}.

In this context, it should be noted that different carbon nanotubes have different dispersion character owing to their surface properties. Clark et al. stated that surfactant assisted dispersion of MWCNTs in an aqueous media is strongly dependent on diameter suggesting that information obtained by examining SWNTs dispersions may not apply to MWCNTs dispersions [7] and vice versa. For example, Cetymethylammonium bromide (CTABr) can be an effective dispersant for SWCNT dispersion in aqueous environments [22]. On the other hand this dispersant did not provide dispersion process of MWCNTs in IPA when it was tried along with SDBS in preliminary experiments by the authors. In this context, this concentration ratios for stability retention is not universal, but confirmed working only on studied variety of MWCNTs.

It should be noted that there is a drawback of calculating concentrations by using absorption spectra. Because absorption of electromagnetic radiation is dependent on state of agglomeration of carbon

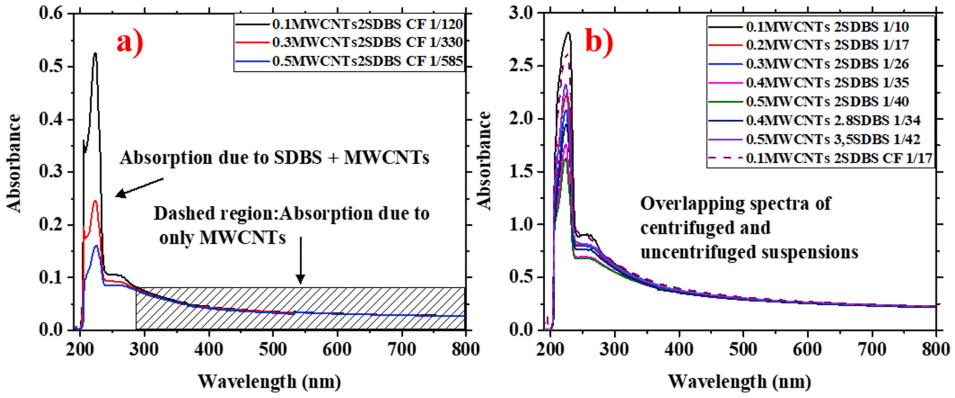


Fig. 3. (a) UV–Vis–NIR absorption spectra of uncentrifuged ultrasonicated SDBS/MWCNTs suspensions in IPA, which are containing almost the same amount of MWCNTs in diluted state, (b) spectra overlapping implemented on centrifuged and uncentrifuged suspensions. Legends refers to amount of dilution. For instance, 0.1MWCNTs2SDBS CF was diluted 120 times.

nanotubes. Giordani et al. stated that agglomerated nanotubes exhibit lower extinction coefficients [40]. Uncentrifuged samples always contain more agglomerated or bundled nanotubes compared to centrifuged ones. Thereby, overlapping an uncentrifuged samples' spectrum with that of centrifuged one yields an overestimated result while predicting MWCNTs concentration in centrifuged suspension. Therefore, MWCNTs concentrations present in Table 1 are believed to be slight overestimates.

3.3. Determination of SDBS concentration by subtraction of UV–Vis spectra

Simplicity of determination of material concentration in the supernatant through a calibration curve is appealing. In this context, it is also used as a tool to determine SDBS concentration in suspensions. SDBS has a benzene ring in its structure where two absorption bands at ~223 nm and ~254 nm are present in IPA. UV–Vis absorption peak at 223 nm was used for plotting calibration curve of SDBS in IPA as shown in Fig. 4a. Corresponding calibration curve is also shown as inset.

CNTs exhibit broad absorptions seen at the UV region due to plasmon resonances in the free electron cloud of π electrons [39]. This peak is reported to be near 248 nm [41]. Absorptions of both SDBS and MWCNTs overlap at the UV region.

Generally for dispersion characterizations, due to this interferences, appropriate wavelengths could be selected [42], but determination of material concentration from overlapping spectra could be complex. In this context, differential spectra were employed in this study. Similar approach has been used in the literature, where interactions of CNTs with various polymeric and biological species were identified by using differential spectra [19–21]. Absorption of photons extends to visible/NIR region for MWCNTs where no distinct signal is present for SDBS. In the far UV, visible and near infrared (NIR) region of spectrum of COOH/MWCNTs suspensions were overlapped with centrifuged spectra of SDBS/MWCNTs suspensions (Fig. 4b). Subtraction yielded differential bound spectra of SDBS, as shown in Fig. 4c.

It was also found that properly diluted spectra of 0.3MWCNTs2SDBS (195 times diluted suspension), 0.4MWCNTs2.8SDBS (255 times diluted suspension) and 0.5MWCNTs3.5SDBS (315 times diluted suspension) are overlapping not only in the visible and near infrared regions, but also in the UV region. This is an expected finding since they are known to contain same SDBS/MWCNTs mass ratio.

For the sake of reliability of concentration determination with bound spectra, overlapping spectrum of COOH/MWCNTs with those of uncentrifuged suspensions were prepared and evaluated as shown in Fig. 4d. It is revealed that especially in the UV region, spectra does not fit perfectly unlike observed on centrifuged suspensions' spectra. This mismatch is obviously reflected in calculated concentrations of these suspensions, which will be explained later.

Absorbance values of bound spectra were used to calculate SDBS concentrations in suspensions (Table 2). It is known that concentration determination through bound spectra can be elaborate. A feature common to all stacked chromophores is hypochromicity, where a stacked dimer structure has less absorbance than sum of its two isolated components [20]. Thereby, if this phenomenon prevails, the process can be expected to display underestimated concentration values. To corroborate; uncentrifuged suspensions (0.1MWCNTs2SDBS CF, 0.3MWCNTs2SDBS CF, 0.5MWCNTs2SDBS CF) were also evaluated in this respect. It appears that calculated concentration values of already known SDBS concentrations of uncentrifuged suspensions are more or less close to accurate values. Because our main aim is to determine whether a peak shift is present, it provides an information that neither hypochromic shifts nor hyperchromic shifts are present in uncentrifuged SDBS/MWCNTs suspensions.

In terms of deviation from actual values (2 g L^{-1}) for uncentrifuged suspensions, two things may prevail: lights passing through is attenuated under the presence of particles in a liquid due to scattering or mass errors from measuring of such low weight of suspensions. Scattering can cause distortion in the spectra and the results are inclined to give wrong estimations. In fact, attenuation of light contains not only information about the energy levels of the absorbing species, but also the particle size distribution in the suspensions. Rayleigh

Table 1
Calculated weight concentrations and ratios in centrifuged and uncentrifuged suspensions by correlation of results of UV–Vis absorption spectroscopy and sediment weighing.

Material	MWCNTs concentration before centrifugation (g L^{-1})	Concentration of precipitate (moisture absorption is neglected) (g L^{-1})	MWCNTs Concentration in supernatant (g L^{-1}), (method: overlapping UV–Vis spectra)	SDBS Concentration in supernatant (g L^{-1})	Initial SDBS/MWCNTs weight concentration ratio (before centrifugation)	Final SDBS/MWCNTs weight concentration ratio (after centrifugation)
0.1MWCNTs2SDBS	0.1	0.535 ± 0.035	0.059	1.505 ± 0.023	20	25.954
0.2MWCNTs2SDBS	0.2	0.670 ± 0.014	0.100	1.428 ± 0.008	10	14.283
0.3MWCNTs2SDBS	0.3	0.720 ± 0.034	0.153	1.423 ± 0.031	6.6	9.305
0.4MWCNTs2SDBS	0.4	0.818 ± 0.05	0.206	1.374 ± 0.044	5	6.674
0.5MWCNTs2SDBS	0.5	0.890	0.235	1.371	4	5.828
0.4MWCNTs2.8SDBS	0.4	0.970 ± 0.014	0.200	2.027 ± 0.007	7	10.133
0.5MWCNTs3.5SDBS	0.5	1.213 ± 0.004	0.247	2.540 ± 0.003	7	10.279

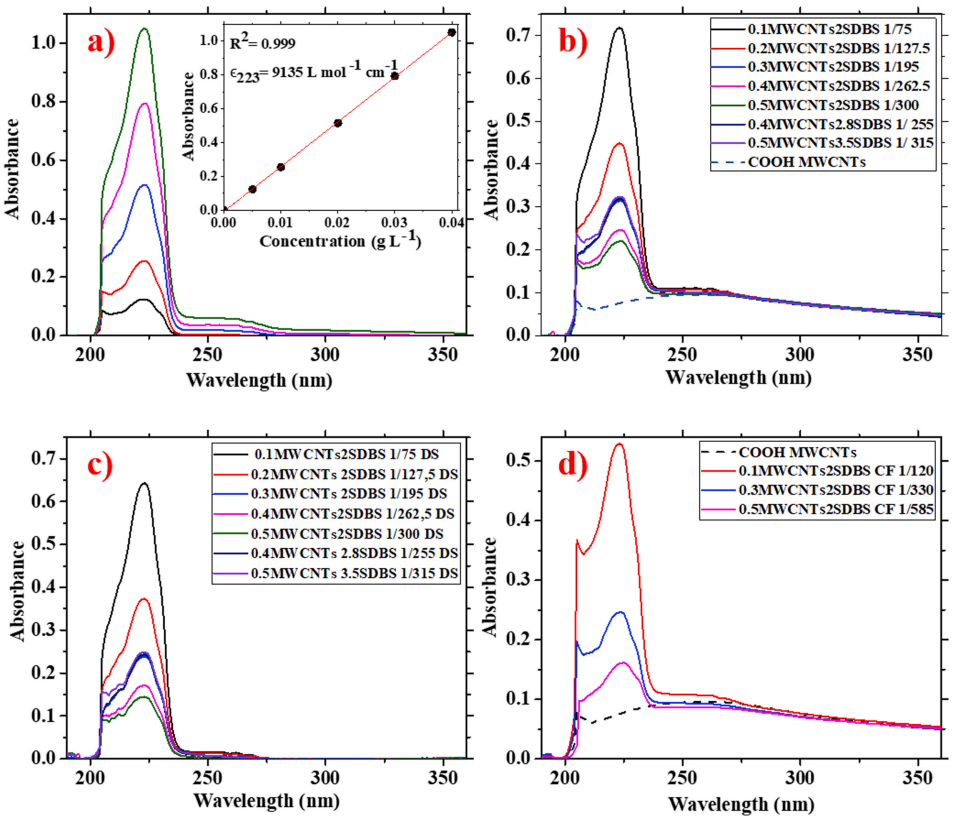


Fig. 4. (a) UV–Vis absorption spectra of SDBS in IPA and inset is corresponding calibration curve drawn by using optical density values at 223 nm, (b) UV absorption spectra of centrifuged dilute MWCNTs suspensions stabilized with SDBS. Suspensions were superimposed in most of the UV, entire visible and NIR range to provide same amount of MWCNTs' presence in diluted suspensions. Overlapping spectrum of diluted COOH/MWCNTs is also represented. (c) is differential spectra (DS) between that of SDBS modified MWCNTs and COOH/MWCNTs. (d) is overlapping spectra of uncentrifuged SDBS/MWCNTs suspensions with that of COOH/MWCNTs'.

Table 2
SDBS weight concentrations calculated by using a calibration curve and bound spectra of SDBS extracted from that of SDBS/MWCNTs suspensions. Derived "wrong" MWCNTs concentrations are also tabulated to show the result of overestimation of SDBS concentrations.

Suspension	SDBS Concentration (g L^{-1}) (UV–Vis analysis)	Calculated MWCNTs concentration (g L^{-1})
0.1MWCNTs2SDBS CF	2.080 ± 0.035	–
0.3MWCNTs2SDBS CF	2.152 ± 0.013	–
0.5MWCNTs2SDBS CF	1.890 ± 0.028	–
0.1MWCNTs2SDBS	1.839 ± 0.003	− 0.274
0.2MWCNTs2SDBS	1.817 ± 0.007	−0.287
0.3MWCNTs2SDBS	1.775 ± 0.020	−0.195
0.4MWCNTs2SDBS	1.716 ± 0.044	−0.134
0.5MWCNTs2SDBS	1.656 ± 0.059	− 0.046
0.4MWCNTs2.8SDBS	2.367 ± 0.026	−0.137
0.5MWCNTs3.5SDBS	2.992 ± 0.039	−0.405

scattering occurs when the diameter of the particle is less than one tenth of the wavelength of the incident radiation. Mie scattering occurs when the particle size is equal to or greater than the incident wavelength. Forward scattering dominates over backscattering as the particle size increases in Mie scattering unlike isotrophic Rayleigh scattering [43]. To surmount this scattering problem an integrating sphere could be used as in the study of Priya et al. [10].

Calculated concentration of SDBS in centrifuged suspensions and derived MWCNTs concentrations reveal that it is impossible to reach accuracy just by using bound SDBS spectra and calibration curves. The results are overestimated compared to the results of UV–Vis-precipitate analysis. Besides, the ratios between UV–Vis analysis and UV–Vis-precipitate analysis results are similar for all suspensions. This dictates that the underlying factor is common to all suspensions. Extinction due to scattering loses may contribute, but it cannot be considered the explaining factor for overestimated results. Because at least gathered information by studying uncentrifuged suspensions is against to this estimation. The cause is not clearly understood, but it may be resulting from several reasons. Presence of functional groups on COOH/MWNCTS may have caused peak shift in π-plasmon region of MWCNTs and hence there may be unobservable/undetectable differences in terms of absorbance between bound MWCNTs spectra in SDBS/MWCNTs and spectrum of COOH/MWCNTs. This contradiction could be arising from diameter dependency of energy of absorption. Supporting information about this is the Rance et al.'s study [39]. It revealed that π-plasmon resonance peak maximums position and energy of absorption are related to diameter of SWCNTs. They have estimated from calculations that as curvature of graphene sheet decreases, energy absorbance decreases as well. This leads us to a conclusion that centrifugation with SDBS may have selected larger diameter MWCNTs. The ones which are better interacting with SDBS molecules should have remained in suspensions while others migrated to precipitate. This should have caused an optical difference between COOH/MWCNTs and MWCNTs in SDBS/MWCNTs suspensions. Eventually, the mismatch of absorbance related to MWCNTs in two different suspensions may have yielded an overestimated SDBS concentrations. In this context, it is expected that COOH/MWCNTs should have lower extinction coefficient compared to MWCNTs in centrifuged SDBS suspensions.

Uncentrifuged suspensions are expected to exhibit larger aggregates than centrifuged suspension. In terms of Mie scattering, smaller particles of centrifuged suspensions have lower forward scattering probability than the particles in uncentrifuged suspensions. Therefore, scattering losses for smaller particles should be lower, which translates into increased absorbance. This may also contribute to overestimation. Several assumptions could be made like listed above, but the real cause is remaining to be unexplained.

3.4. Zeta potential and particle size analysis

ELS can be employed for dispersion characterization which measures velocity of the particles in the suspension. Through this

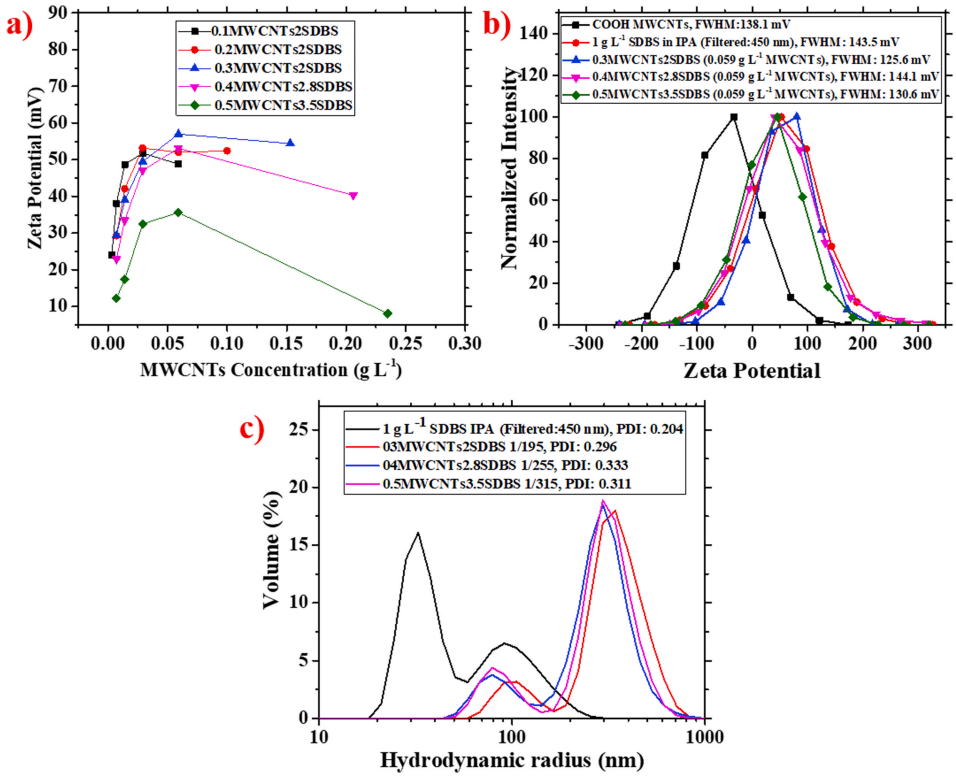


Fig. 5. (a) Zeta potential values of SDBS modified MWCNTs suspensions in IPA as a function of MWCNTs concentration, (b) zeta potential distribution curves of selected suspensions, (c) volume based particle size distribution curves of suspensions (dilution factors are included in legends).

information, electrophoretic mobility of particles and eventually zeta potential could be calculated. Zeta potential analysis is a reliable stability characterization technique [38] as it gives a quantitative information about generated repulsion between particles with the help of electrical double layers surrounding them, which in turn yields useful information about suspensions stability. In addition, when particles are aggregated the mass of the particles increases, and they move slowly, leading to a smaller zeta potential [36]. Therefore, zeta potential may also yield information about aggregation, and a larger zeta potential may mean there is a better dispersion.

Fig. 5a shows chance in zeta potential as a function of MWCNTs weight concentration in supernatants. It should be noted that as produced CNTs have a small and positive zeta potential [44]. SDBS molecules bind to the liquid-MWCNTs interface due to π-π stacking interactions, hence MWCNTs aggregates exhibit exceptionally higher zeta potential values than pristine MWCNTs. Our observation revealed that head groups of ($-SO^{3-}Na$) SDBS molecules remain undissociated in IPA. Thereby, SDBS modified MWCNTs suspensions show positive sign of charge. Initial dilutions were all carried out to reach 0.059 g L^{-1} MWCNTs, then series of dilutions were conducted each time to reach half the amount of previous one. It seems that almost for every suspension (except 0.2MWCNTs2SDBS) zeta potential reaches a plateau value at a particular concentration and then it dwindles as dilution proceeds. It is understood that as prepared supernatants contain high amount of particulate matter that it causes overlapping of double layers around particles-aggregates. Appropriate dilution causes relief of confined electrical double layers and zeta potential increases.

Highest observed zeta potential was reached at $+57.0 \pm 0.63$ mV with 0.3MWCNTs2SDBS when MWCNTs concentration was 0.059 g L^{-1} and the value was $+54.4 \pm 0.99$ mV for undiluted 0.3MWCNTs2SDBS suspension (0.153 g L^{-1} MWCNTs containing sample). Generally stability is considered maintained when a threshold of +30 mV or −30 mV is reached [35]. Thus, in this study most of the suspensions (except 0.5MWCNTs3.5SDBS) can be considered stable even when they are in undiluted state.

Due to the probability of higher number of surfactants on MWCNTs surfaces responsible for charge generation, one might expect that a higher magnitude of zeta potential should be obtained with 0.1MWCNTs2SDBS and 0.2MWCNTs2SDBS. On the contrary, they were slightly less stable. Similarly, Blanch et al. found out that higher surfactant concentrations inducing a faster rate of flocculation [33] due to attractive depletion type interactions among surfactant micelles.

At first glance considering results of sedimentation tests, 0.4MWCNTs2.8SDBS and 0.5MWCNTs3.5SDBS suspensions should be expected to have higher zeta potential values. However, their sedimentation rate is slower than 0.3MWCNTs2SDBS. Because, in addition to the effect of repulsion between particles, sedimentation rate of a suspension can be opposed by (i) decrease in particle size, (ii) increase in viscosity of the suspensions and (iii) matching the density between solvents and solid phases. We attribute this slower sedimentation rate, but lower zeta potential to mainly increase in viscosity of suspensions. Because size distribution of these suspensions are almost the same according to DLS data, which will be explained later.

Fig. 5b shows zeta potential distribution curves of selected SDBS/MWCNTs suspensions with highest observed zeta potential values for the respective SDBS/MWCNTs system. The most important aspect common to all zeta potential distribution curves is broadness. Broad distribution curves were also observed by White et al. [29] and Sun et al. [38] on both nanotube/surfactant containing or only surfactant containing solutions. Sun et al. [38] argued that it is unlikely to put forward that they observe electrophoretic mobility of micelles not nanotubes. To investigate this, we also conducted zeta potential analysis on COOH/MWCNTs which are free from surfactants. Zeta potential distribution curves of COOH/MWCNTs is also broad indicating that nanotubes are contributing to electrophoretic mobility and peak broadening as well. The peak broadening may be originating from several aspects. Firstly, the reason could be the low signal to noise ratio of the zeta potential measurements. This becomes pronounced in

concentrated suspensions. Even though it is observed that concentration has an influence on peak broadening (not shown), it is not the only underlying factor since we also observed considerably broad peaks on diluted samples' zeta potential distribution curves as well. The second reason could be resulting from variation in diameters and chiralities of MWCNTs or different shapes of micelles present in solutions being analyzed [29]. It is known that ultrasonication causes fragmentation of MWCNTs. MWCNTs with varying in length may also contribute to peak broadening. Interestingly zeta potential distribution curves of suspensions are symmetrical, therefore at first glance it suggests that the system may be composed of similar sized aggregates. Because Lee et al. dealt with similar problem and observed bimodal zeta potential distribution on sodium dodecyl benzene sulfonate (SDS) modified SWCNTs suspensions [36].

To make a correlation with zeta potential analysis and to investigate agglomeration and interaction behavior of SDBS and MWCNTs, DLS analysis were also conducted. It should be noted that DLS analysis could be conducted under normal mode or under high resolution mode. Upon observing bimodal size distribution in preliminary experiments under normal mode, high resolution analysis were presented in this work which is appropriate if one wants to better resolve size distribution data of different entities in suspensions. Both pure SDBS and SDBS/MWCNTs suspensions have bimodal size distribution as shown in Fig. 5c. Polydispersity index (PDI) values also indicate that the size distribution is broad. Matarredona et al. postulated that surfactants adsorb on external surface of nanotubes, as a result the nanotube-surfactant aggregate takes indeed the appearance of a cylindrical micelle with nanotube resting in the interior [42]. In our case, it is likely to happen, but probably first layer of SDBS molecules rest on MWCNTs surfaces horizontally by attaching their benzene rings to nanotube surface. Once the monolayer is formed consecutive randomly oriented adsorptions eventually cause formation of high aspect ratio core-shell particles. High power ultrasonication causes MWCNTs to have different lengths, which may also contribute to the observed bimodal size distribution. However, bimodal size distribution is preserved in SDBS suspensions. This may imply that an individual MWCNT or bundles of MWCNTs can be encapsulated in cylindrical micelles of surfactants as suggested in the study of O'Connell et al. [45]. It should be noted that particle size distributions of MWCNTs are ranging from around 50 nm to 800 nm. This broad size distribution implies that MWCNTs are fragmented and in bundled form as shown in Fig. 1b. It could also be deduced from DLS observations that aggregation behaviors of MWCNTs in investigated samples are similar. However, 0.4MWCNTs2.8SDBS and 0.5MWCNTs3.5SDBS provides slightly better dispersion compared to 0.3MWCNTs2SDBS, since their peaks are shifted to lower particle sizes. It should be noted that when considering particle size distribution, one should be aware of the fact that the extracted information from DLS is a projection of a sphere having the same translational diffusion coefficient as the particles in the suspension. If cylindrical micelles and nanotubes are present, this information needs to be considered.

Although DLS shows a bimodal size distribution, zeta potential distribution does not exhibit bimodal distribution. However, it can be put forward that results correlate with each other. Because ELS distribution is broad as expected which may be the reflection of broad size distribution of aggregates in the suspensions as aforementioned. In terms of effect of increment in SDBS or MWCNTs concentrations in suspensions, both observations' results are similar. They exhibit almost the same full width half maximum (FWHM) values for zeta potential distribution curves and similar size distribution curves.

4. Conclusion

The present study deals with dispersion of MWCNTs via SDBS in IPA by employing ultrasonication-centrifugation. The effect of SDBS/MWCNTs ratios in supernatants on obtaining stable suspensions containing CNTs is also addressed. UV–Vis absorption spectroscopy, sedimentation tests, zeta potential and dynamic light scattering analysis were used as tools to estimate the optimal multi walled carbon nanotube (MWCNTs)/dispersant weight ratio in stable suspensions and to evaluate state of dispersion.

Overlapping UV–Vis spectra of centrifuged and uncentrifuged suspensions is enabled calculation of MWCNTs concentrations in supernatants, additionally information gathered from sediment weights of centrifuged suspensions enabled the estimation of SDBS/MWCNTs mass ratios in supernatants. It is found that SDBS/MWCNTs concentrations ratio should be at least 6.6 before centrifugation in order to achieve stability in the SDBS/MWCNTs suspension. It is also found that increasing SDBS/MWCNTs concentrations in supernatants gradually decreases the zeta potentials among compared suspensions which in turn decreases settling velocity and sedimentation rate, which may be attributed to the increase in viscosity of supernatants. Differential or bound spectra of SDBS in supernatants exhibit an unexpected hyperchromic shifts at λ_{max} causing inaccurate concentration estimations. Although the cause of inaccurate estimations is still unclear; interpretations are presented in the article.

A deeper understanding is crucial for every composite system (like dispersant stabilized ceramic suspensions) when intended to be analyzed with UV–Vis spectroscopy, which is the diagnosis for interaction of materials with electromagnetic waves or influence of one constituent to other's optical property. Namely, notwithstanding this article present a specific case of a composite suspension system, crucial information is provided as a guideline for the proper diagnosis process of other systems to extract reliable data.

Declaration of competing interest

The authors declare that they have no known competing financial interests or personal relationships that could have appeared to influence the work reported in this paper.

Acknowledgements

This research was financed by TUBITAK (The Scientific and Technological Research Council of Turkey under the grant number of 109R007).

References

[1] A.-E. Hsiao, S.-Y. Tsai, M.-W. Hsu, S.-J. Chang, Decoration of multi-walled carbon nanotubes by polymer wrapping and its application in MWCNT/polyethylene composites, Nanoscale Res. Lett. 7 (2012) 240, https://doi.org/10.1186/1556-276X-7-240.

[2] F. Inam, A. Heaton, P. Brown, T. Peijs, M.J. Reece, Effects of dispersion surfactants on the properties of ceramic-carbon nanotube (CNT) nanocomposites, Ceram. Int. 40 (2014) 511–516, https://doi.org/10.1016/j.ceramint.2013.06.031.

[3] A. Sobolkina, V. Mechtcherine, V. Khavrus, D. Maier, M. Mende, M. Ritschel, A. Leonhardt, Dispersion of carbon nanotubes and its influence on the mechanical properties of the cement matrix, Cem. Concr. Compos. 34 (2012) 1104–1113, https://doi.org/10.1016/j.cemconcomp.2012.07.008.

[4] A. Thess, R. Lee, P. Nikolaev, H. Dai, P. Petit, J. Robert, C. Xu, Y.H. Lee, S.G. Kim, A.G. Rinzler, D.T. Colbert, G.E. Scuseria, D. Tomanek, J.E. Fischer, R.E. Smalley, Crystalline ropes of metallic carbon nanotubes, Science 273 (1996) 483–487, https://doi.org/10.1126/science.273.5274.483.

[5] S.D. Bergin, Z. Sun, D. Rickard, P.V. Streich, J.P. Hamilton, J.N. Coleman, Multicomponent solubility parameters for single-walled carbon Nanotube − Solvent mixtures, ACS Nano 3 (2009) 2340–2350, https://doi.org/10.1021/nn900493u.

[6] M. Monthioux, B.W. Smith, B. Burteaux, a. Claye, J.E. Fischer, D.E. Luzzi, Sensitivity of single-wall carbon nanotubes to chemical processing: an electron microscopy investigation, Carbon N. Y. 39 (2001) 1251–1272, https://doi.org/10.1016/S0008-6223(00)00249-9.

[7] M.D. Clark, S. Subramanian, R. Krishnamoorti, Understanding surfactant aided aqueous dispersion of multi-walled carbon nanotubes, J. Colloid Interface Sci. 354 (2011) 144–151, https://doi.org/10.1016/j.jcis.2010.10.027.

[8] a.G. Osorio, I.C.L. Silveira, V.L. Bueno, C.P. Bergmann, H2SO4/HNO3/HCl-Functionalization and its effect on dispersion of carbon nanotubes in aqueous media, Appl. Surf. Sci. 255 (2008) 2485–2489, https://doi.org/10.1016/j.apsusc.2008.07.144.

[9] Y.T. Shieh, G.L. Liu, H.H. Wu, C.C. Lee, Effects of polarity and pH on the solubility

of acid-treated carbon nanotubes in different media, Carbon N. Y. 45 (2007) 1880–1890, https://doi.org/10.1016/j.carbon.2007.04.028.
[10] B.R. Priya, H.J. Byrne, Investigation of sodium dodecyl benzene sulfonate assisted dispersion and debundling of single-wall carbon nanotubes, J. Phys. Chem. C 112 (2008) 332–337, https://doi.org/10.1021/jp0743830.
[11] R. Rastogi, R. Kaushal, S.K. Tripathi, A.L. Sharma, I. Kaur, L.M. Bharadwaj, Comparative study of carbon nanotube dispersion using surfactants, J. Colloid Interface Sci. 328 (2008) 421–428, https://doi.org/10.1016/j.jcis.2008.09.015.
[12] T. Hasan, V. Scardaci, P. Tan, A.G. Rozhin, W.I. Milne, A.C. Ferrari, Stabilization and “debundling” of single-wall carbon nanotube dispersions in N-methyl-2-pyrrolidone (NMP) by polyvinylpyrrolidone (PVP), J. Phys. Chem. C 111 (2007) 12594–12602, https://doi.org/10.1021/jp0723012.
[13] Y.L. Zhao, J.F. Stoddart, Noncovalent functionalization of single-walled carbon nanotubes, Acc. Chem. Res. 42 (2009) 1161–1171, https://doi.org/10.1021/ar900056z.
[14] L. Vaisman, H.D. Wagner, G. Marom, The role of surfactants in dispersion of carbon nanotubes, Adv. Colloid Interface Sci. 128–130 (2006) 37–46, https://doi.org/10.1016/j.cis.2006.11.007.
[15] S. Utsumi, M. Kanamaru, H. Honda, H. Kanoh, H. Tanaka, T. Ohkubo, H. Sakai, M. Abe, K. Kaneko, RBM band shift-evidenced dispersion mechanism of single-wall carbon nanotube bundles with NaDDBS, J. Colloid Interface Sci. 308 (2007) 276–284, https://doi.org/10.1016/j.jcis.2006.12.041.
[16] M.F. Islam, E. Rojas, D.M. Bergey, a.T. Johnson, a.G. Yodh, High weight fraction surfactant solubilization of single-wall carbon nanotubes in water, Nano Lett. 3 (2003) 269–273, https://doi.org/10.1021/nl025924u.
[17] J. Njuguna, O.A. Vanli, R. Liang, A review of spectral methods for dispersion characterization of carbon nanotubes in aqueous suspensions, J. Spectrosc. 2015 (2015), https://doi.org/10.1155/2015/463156.
[18] Y. Shi, Optimization conditions for single-walled carbon nanotubes dispersion, J. Surf. Eng. Mater. Adv. Technol. (2013) 6–12, https://doi.org/10.4236/jsemat.2013.31002 03.
[19] V.A. Karachevtsev, A.M. Plokhotnichenko, M.V. Karachevtsev, V.S. Leontiev, Decrease of carbon nanotube UV light absorption induced by pi–pi-stacking interaction with nucleotide bases, Carbon N. Y. 48 (2010) 3682–3691, https://doi.org/10.1016/j.carbon.2010.06.009.
[20] M.E. Hughes, E. Brandin, J.A. Golovchenko, Optical absorption of DNA − carbon nanotube structures, Nanto Lett 7 (2007) 1191–1194.
[21] O.H. Cha, M.S. Jeong, C.C. Byeon, H. Jeong, J.H. Han, Y. Chul, K.H. An, K. Oh, K.K. Kim, Y.H. Lee, Relative content evaluation of single-walled carbon nanotubes using, UV-VIS-NIR Absorption Spectroscopy 10 (2009) 9–13.
[22] S. Attal, R. Thiruvengadathan, O. Regev, Determination of the concentration of single-walled carbon nanotubes in aqueous dispersions using UV-visible absorption spectroscopy, Anal. Chem. 78 (2006) 8098–8104.
[23] Y. Ye, S. Cai, M. Yan, T. Chen, T. Guo, Concentration detection of carbon nanotubes in electrophoretic suspension with UV-vis spectrophotometry for application in field emission devices, Appl. Surf. Sci. 284 (2013) 107–112, https://doi.org/10.1016/j.apsusc.2013.07.037.
[24] S.H. Jeong, K.K. Kim, S.J. Jeong, K.H. An, S.H. Lee, Y.H. Lee, Optical absorption spectroscopy for determining carbon nanotube concentration in solution, Synth. Met. 157 (2007) 570–574, https://doi.org/10.1016/j.synthmet.2007.06.012.
[25] J.L. Bahr, E.T. Mickelson, M.J. Bronikowski, R.E. Smalley, J.M. Tour, Dissolution of small diameter single-wall carbon nanotubes in organic solvents? Chem. Commun. (2001) 193–194, https://doi.org/10.1039/b008042j.
[26] R.M.F. Fernandes, B. Abreu, B. Claro, M. Buzaglo, O. Regev, I. Fur, E.F. Marques, Dispersing carbon nanotubes with ionic surfactants under controlled conditions: comparisons and insight, Langmuir 31 (2015) 10955–10965, https://doi.org/10.1021/acs.langmuir.5b02050.
[27] A.C. Zaman, C. Kaya, Determination of quantity of materials in suspensions and in electrophoretic coatings by UV-visible absorption spectroscopy, J. Electrochem. Soc. 162 (2015) D3109–D3111, https://doi.org/10.1149/2.0261511jes.
[28] J. Lee, M. Kim, C.K. Hong, S.E. Shim, Measurement of the dispersion stability of pristine and surface-modified multiwalled carbon nanotubes in various nonpolar and polar solvents, Meas. Sci. Technol. 18 (2007) 3707–3712, https://doi.org/10.1088/0957-0233/18/12/005.
[29] B. White, S. Banerjee, S.O. Brien, N.J. Turro, I.P. Herman, Zeta-potential measurements of surfactant-wrapped, Individual Single-Walled Carbon Nanotubes 2 (2007) 13684–13690.
[30] Z.F. Li, G.H. Luo, W.P. Zhou, F. Wei, R. Xiang, Y.P. Liu, The quantitative characterization of the concentration and dispersion of multi-walled carbon nanotubes in suspension by spectrophotometry, Nanotechnology 17 (2006) 3692–3698, https://doi.org/10.1088/0957-4484/17/15/012.
[31] J. Yu, N. Grossiord, C.E. Koning, J. Loos, Controlling the dispersion of multi-wall carbon nanotubes in aqueous surfactant solution, Carbon N. Y. 45 (2007) 618–623, https://doi.org/10.1016/j.carbon.2006.10.010.
[32] P. Alafogianni, K. Dassios, S. Farmaki, S.K. Antiohos, T.E. Matikas, N.M. Barkoula, On the efficiency of UV-vis spectroscopy in assessing the dispersion quality in sonicated aqueous suspensions of carbon nanotubes, Colloids Surfaces A Physicochem. Eng. Asp. 495 (2016) 118–124, https://doi.org/10.1016/j.colsurfa.2016.01.053.
[33] A.J. Blanch, C.E. Lenehan, J.S. Quinton, Optimizing surfactant concentrations for dispersion of single-walled carbon nanotubes in aqueous solution, J. Phys. Chem. B 114 (2010) 9805–9811, https://doi.org/10.1021/jp104113d.
[34] A.G. Hsieh, S. Korkut, C. Punckt, I. a Aksay, Dispersion stability of functionalized graphene in aqueous sodium dodecyl sulfate solutions, Langmuir 29 (2013) 14831–14838, https://doi.org/10.1021/la4035326.
[35] ASTM, Standard Guide for Measurement of Electrophoretic Mobility and Zeta Potential of Nanosized Biological Materials, (2013), pp. 1–7, https://doi.org/10.1520/E2865-12.2.
[36] J.Y. Lee, J.S. Kim, K. Hyeok An, K. Lee, D.Y. Kim, D.J. Bae, Y.H. Lee, Electrophoretic and dynamic light scattering in evaluating dispersion and size distribution of single-walled carbon nanotubes, J. Nanosci. Nanotechnol. 5 (2005) 1045–1049, https://doi.org/10.1166/jnn.2005.160.
[37] V.C. Moore, M.S. Strano, E.H. Haroz, R.H. Hauge, R.E. Smalley, J. Schmidt, Y. Talmon, Individually suspended single-walled carbon nanotubes in various surfactants, Nano Lett. 3 (2003) 1379–1382, https://doi.org/10.1021/nl034524j.
[38] Z. Sun, V. Nicolosi, D. Rickard, S.D. Bergin, D. Aherne, J.N. Coleman, Quantitative evaluation of surfactant-stabilized single-walled carbon Nanotubes:\nDispersion quality and its correlation with zeta potential, J. Phys. Chem. C 112 (2008) 10692–10699.
[39] G.a. Rance, D.H. Marsh, R.J. Nicholas, A.N. Khlobystov, UV–vis absorption spectroscopy of carbon nanotubes: relationship between the π-electron plasmon and nanotube diameter, Chem. Phys. Lett. 493 (2010) 19–23, https://doi.org/10.1016/j.cplett.2010.05.012.
[40] S. Giordani, S.D. Bergin, V. Nicolosi, S. Lebedkin, M.M. Kappes, W.J. Blau, J.N. Coleman, Debundling of single-walled nanotubes by dilution: observation of large populations of individual nanotubes in amide solvent dispersions, J. Phys. Chem. B 110 (2006) 15708–15718, https://doi.org/10.1021/jp0626216.
[41] J.H. Lehman, M. Terrones, E. Mansfield, K.E. Hurst, V. Meunier, Evaluating the characteristics of multiwall carbon nanotubes, Carbon N. Y. 49 (2011) 2581–2602, https://doi.org/10.1016/j.carbon.2011.03.028.
[42] O. Matarredona, H. Rhoads, Z. Li, J.H. Harwell, L. Balzano, D.E. Resasco, Dispersion of single-walled carbon nanotubes in aqueous solutions of the anionic surfactant NaDDBS, J. Phys. Chem. B 107 (2003) 13357–13367, https://doi.org/10.1021/jp0365099.
[43] K. Arepalli, S. Freiman, S.W. Hooker, S. Migler, Measurement issues in single-wall carbon nanotubes, http://www.nist.gov/manuscript-publication-search.cfm?pub_id=852726, (2008) 72.
[44] A.R. Boccaccini, J. Cho, J.a. Roether, B.J.C. Thomas, E. Jane Minay, M.S.P. Shaffer, Electrophoretic deposition of carbon nanotubes, Carbon N. Y. 44 (2006) 3149–3160, https://doi.org/10.1016/j.carbon.2006.06.021.
[45] M.J. O'Connell, S.M. Bachilo, C.B. Huffman, V.C. Moore, M.S. Strano, E.H. Haroz, K.L. Rialon, P.J. Boul, W.H. Noon, C. Kittrell, J. Ma, R.H. Hauge, R.B. Weisman, R.E. Smalley, Band gap fluorescence from individual single-walled carbon nanotubes, Science 297 (2002) 593–596, https://doi.org/10.1126/science.1072631.